HTS Cable and Protection System Study for UK's 275 kV Transmission Network

Pavan Chaganti, Kevin Kawal, Qiteng Hong, Weijia Yuan, Min Zhang, Arnaud Allais, Jean-Maxime Saugrain, Anne Pochylski, Beate West, Nicolas Lallouet, Mike Ross and Sean Coleman

***Abstract*— The global shift towards zero carbon emissions has led to an increased demand for electricity, (e.g. For electrification of heat, transportation, etc.). High-temperature superconductor (HTS) cables offer a high-capacity and small-footprint solution compared to traditional cable technologies, making them ideal for densely populated areas. HTS cables, however, possess different electrical characteristics compared to conventional cables. This paper presents a specific case study of a 12.9 km long 275 kV HTS cable connecting Birkenhead Substation and Lister Drive Substation in the UK. A dynamic electrical model incorporating the varying resistance of the HTS cable was constructed. The HTS cable model was integrated into an equivalent test network, representing conditions at the target site, to analyse its behaviour and impact on conventional power system protection performance via simulation case studies. The results indicate that differential protection operates reliably, while distance protection is impacted by the varying resistance. However, the proposed HTS cable design at the specified location presents a relatively small change in HTS cable resistance. The impact on distance protection was therefore minimal and can be addressed by considering HTS properties when determining distance protection settings. The study was conducted by considering manufacturer-supplied HTS parameters, network parameters reflective of an actual location in the UK grid, and protection requirements specified in the UK grid code. The study provides valuable insights into practicality and protection strategies for reliable HTS cable operation in a real-world transmission network. The findings can inform future HTS cable designs and installations globally, as well as provide a framework for further research in this area.**

***Index Terms*— HTS cable, Faults, distance, and differential relay.**

I. INTRODUCTION

Superconductor power cables have been gaining attention due to their high power density and low losses [1]–[4]. This feature is particularly advantageous in densely populated areas as it eliminates the need for more electrical equipment installations and the construction of new substations [5]. Additionally, with the electrification of transport and heating, there will be a significant increase in demand in densely populated areas like city centers, and recent techno-economic studies have shown that HTS cables combined with advancements in cooling technologies can offer a cost effective solution in meeting such increased demand [6]–[10]. In the event of a fault within a power system utilizing HTS cables, instantaneous fault current leads to a temperature rise where the superconductor resistance changes, possibly leading to quenching, depending on the design of the cable, as well as potential damage to the superconducting tapes. Power system protection should operate reliably under fault conditions and isolate the faulted section of the network, in order to maintain safety, prevent further equipment damage, and maintain network stability. However, the non-linear change in the resistance of superconductor cables also poses challenges for conventional protection schemes and coordination [11].

However, it should be noted, that in real-world applications the quench mode is not typically utilized, and a copper former provides a conduction path for fault current. HTS properties are therefore dependent upon factors such as cable design and network configuration. The fault current characteristics will also be influenced by the change in impedance characteristics between the superconducting mode and the fault conduction mode (either copper conduction or quenching). Such changes in fault levels and fault characteristics can potentially impact typically adopted AC protection methods, potentially leading to maloperation and thus threatening the reliable and secure operation of the power network. It is therefore critical to investigate the fault characteristics of HTS cables and assess the impacts of variable HTS cable impedance on typically adopted AC protection methods. A summary of the effects of HTS cables on different protection methods is presented in Table 1.

Table 1 Review of HTS cable influence on the protection techniques

Protection technique	Quenching (Y/N)	Key Findings	Ref.
Overcurrent Protection	Y	• Fault Current magnitude is limited during internal/external faults. • Overcurrent relay coordination negatively impacted.	[11], [12]
Differential Protection	Y	• Operates suitably.	[13], [14]
Distance Protection	Y	• Quenching impacts relay performance.	[12], [13]
	N	• Relatively small adverse impacts on distance relay performance. • Backup distance protection was demonstrated for 1km HTS cable.	[14]
Thermal Relay	Y	• Utilizes thermo-electric properties of HTS cable • Provides dependable HTS cable protection.	[13], [15]
Time-domain based methods	Y	• AI-based methods using time domain features. • Robust against time-varying impedance characteristic • Not demonstrated in practical scenarios.	[16]

In the paper, we discuss the distance and differential protection system behaviour during the internal and external

This study was funded by the UK Ofgem's Strategic Innovation Fund. This work is a collaboration with the project partners National Grid Electricity Transmission (NGET), National grid Electricity distribution, UK Power Networks, SP Energy Networks, University of Strathclyde, University of Manchester, Nexans, AMSC Orsted and Frazer-Nash Consultancy. Pavan Chaganti, Kevin Kawal, Qiteng Hong, Weijia Yuan, and Min Zhang are with the University of Strathclyde, Glasgow, G1 1RD, U.K.
Arnaud Allais, Jean-Maxime Saugrain, Anne Pochylski, Beate West, Nicolas Lallouet are with the Nexans, France.
Mike Ross is with the AMSC, Massachusetts, United States
Sean Coleman is with Deeside Centre for Innovation, National Grid, United Kingdom

faults in the 275 kV HTS cable 12.9 km long between the Lister and Birkenhead substations in the UK transmission system and also, the challenges posed by HTS's unique properties.

II. Methodology

In this study, the HTS power cable is composed of three separate individual core HTS superconducting power cables as shown in Fig. 1 and the transposed line diagram of the HTS cables is shown in Fig. 2.

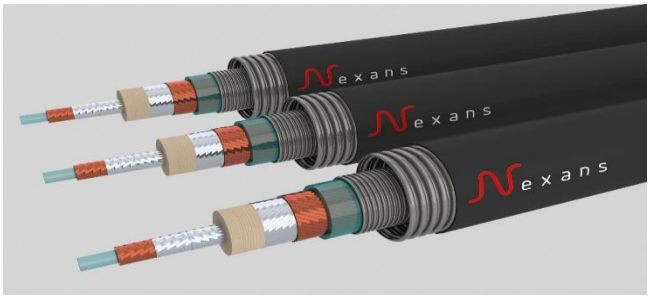

Fig. 1. Three single core High-temperature superconductor power cable

The resistance of the superconductor is evaluated using the E-J Power law:

$$R_{sc} = \frac{E_o}{I_c(T)}\left(\frac{I}{I_c(T)}\right)^n * length \quad [\Omega] \qquad 1$$

The resistance of copper layers or core is given below

$$\rho_{cu} = (-2.46499 + 0.06351 * T)10^{-9} \quad [\Omega.\text{m}] \qquad 2$$

$$R_{cu} = \frac{\rho_{cu} * length}{Area} \qquad 3$$

The critical current which is dependent on the operating temperature of the cable is as follows:

$$I_c = I_c(T_o)\frac{(T_c - T)}{(T_c - T_o)} \qquad 4$$

Where, T_c = 92 K represents the critical temperature, T_o= 67 K denotes the initial temperature, and $I_c(T_o)$ singnifies the critical current at 67 K. T stands for the temperature of tapes and n is equal to 25. The critical electric field $E_o = 1 \times 10^{-4}\, V/m$.

$$I_c(T_o) = \begin{cases} 2730, & for\ HTS\ phase \\ 3000\ A, & for\ HTS\ Screen \end{cases} \qquad 5$$

$$Area = \begin{cases} 240\ mm^2, & for\ \ copper\ Core \\ 245\ mm^2, & for\ \ Screen \end{cases} \qquad 6$$

The phase impedance of the three individual phases; Phase A, phase B, and Phase C impedance are as follows:

$$Z_a = \frac{V_a - V'_a}{I_a} = Z_s + \frac{(Z_m I_b + Z_m I_c)}{I_a} \qquad 7$$

$$Z_b = \frac{V_b - V'_b}{I_b} = Z_s + \frac{(Z_m I_a + Z_m I_c)}{I_b} \qquad 8$$

$$Z_c = \frac{V_c - V'_c}{I_c} = Z_s + \frac{(Z_m I_b + Z_m I_a)}{I_c} \qquad 9$$

The self-impedance of each phase of the cable is as follows:

$$Z_s = (Z_0 + 2Z_1)/3 \qquad 10$$

The mutual impedance of each phase of the cable is as follows:

$$Z_m = (Z_0 - Z_1)/3 \qquad 11$$

Where $X_a, X_b\ and\ X_c$ are the self-reactance of each line and X_m is the mutual reactance between the pair of lines. Where Z_0, Z_1 and Z_2 are the zero, positive, and negative sequence impedance of the superconducting power cable.

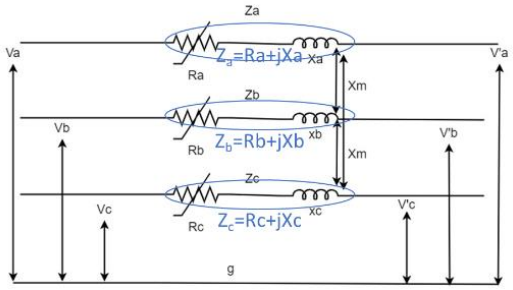

Fig. 2. Transpose line diagram of the HTS cable

In the MATLAB/Simulink environment, we have developed the HTS model and an equivalent test network. Grid connections are represented as equivalent voltage sources accompanied by representative impedances reflecting the relevant fault characteristics. Voltage and current measurements are then fed into relay protection models, which are evaluated under various fault scenarios and locations, encompassing both conventional and HTS cables.

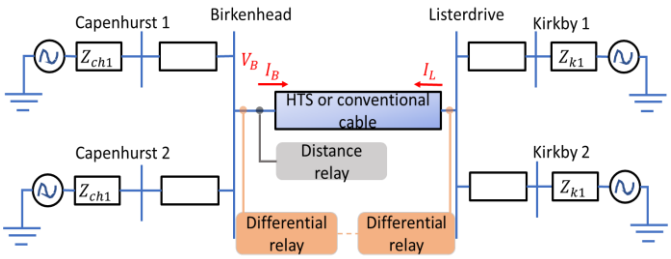

Fig. 3. Schematic view of the network between the Birkenhead and Listerdrive with protection system

Table 2 HTS cable and conventional cable parameters are given by Nexans and National Grid.

Parameter	Value	Unit
Rated Voltage, $V_{L\text{-}L}$ (rms)	275	kV
Superconducting Resistance, R^S_{HTS}	0.0003	Ω/km
Superconducting Inductance, L^S_{HTS}	0.06	mH/km
HTS Capacitance, C_{HTS}	0.2	µF/km
Resistance of Conventional Cable, R_{CC}	0.0142	Ω/km
Inductance of Conventional Cable, L_{CC}	0.51	mH/km
Capacitance of Conventional Cable, C_{cable}	0.332	µF/km
Length of Conventional/HTS Cable, l	12.9	km

The zero, positive, and negative sequences of the superconductor under steady state at 67 K temperature at rated current are 0.0004+1.0117i, 0.000+1.0108i, and 0.0003+1.0108i, respectively. These values are given by Nexans.

The protection standards specified in the UK grid code [17] for 275 kV circuits exceeding a length of 10 km, require

primary unit protection and secondary non-unit protection. Primary unit protection entails a comparison of parameters at the boundaries of the protected zone, while secondary non-unit protection relies on local relay measurements to define protection zones that can be synchronized to serve as backup for other non-unit protection components. In the UK, the primary unit protection and secondary non-unit protection are typically distance protection and current differential, respectively. This document provides detailed insights into the settings and fault considerations associated with both differential and distance protection schemes in the 275-kV circuit.

A. Differential protection setting

In this study, the employed differential protection model follows a commonly used two-slope characteristic, depicted in Fig. 4(a), where it utilizes differential current (I_d) and restraint current (I_r) as defined by equations (12) to (14).

$$I_d = |I_B + I_L| \tag{12}$$

$$I_r = \frac{|I_B| + |I_L|}{2} \tag{13}$$

$$\begin{cases} I_d > k_1 I_r + I_{s1}, & \text{if } I_r^{UGC} \le I_{s2} \\ I_d > k_2 I_r + (k_1 - k_2) I_{s2} + I_{s1}, & \text{If } I_r^{UGC} > I_{s2} \end{cases} \tag{14}$$

Here, I_B and I_L represent the currents entering the protected line from the Birkenhead and Listerdrive ends, respectively. Typical relay settings are adopted as I_{s1} (=1.0 A secondary), the relay minimum pick-up current; I_{s2} (=5.0 A secondary), the point at which the relay slope switches; and k_1(=0.3) and k_2 (=0.15) are the relay bias slopes.

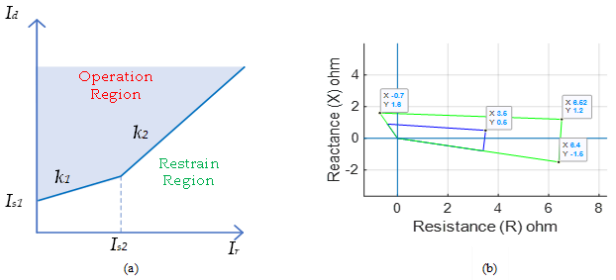

Fig. 4. (a) Differential relay two slope characteristic and (b) Distance relay quad characteristic

B. Distance protection settings

The distance protection principle relies on the measurement of impedance at the relay location, utilizing local voltage and current data. Impedance values are measured for each phase-to-ground and phase-to-phase connection. During fault conditions, the impedance trajectory measured by the relay moves into a pre-defined zone as depicted in Fig. 4(b). The existing distance protection relay employs a quadrilateral characteristic with Zone 1 covering 80% of the protected circuit length and Zone 2 extending to 120% of the protected circuit length. The formulas governing the impedance measurements captured by the relay denoted as Z_{relay} and incorporating the zero-sequence compensation factor K, are elaborated in equations (15)-(17).

$$Z_{relay} = \frac{V_B^{\phi}}{\left(I_B^{\phi} + K I_{res}\right)} \tag{15}$$

$$I_{res} = I_a + I_b + I_c \tag{16}$$

$$K = \frac{1}{3}\left(\frac{Z_{L0}}{Z_{L1}} - 1\right) \tag{17}$$

Here V_B and I_B are the voltage and current measurements taken at the relay location in Birkenhead, while ϕ represents the relevant phase impedance being measured. Z_{L1} and Z_{L0} correspond to the positive and zero sequence impedance values associated with the protected circuit, which may encompass either the conventional cable or the HTS cable.

C. Fault conditions

In our analysis of the cable data, we have considered various scenarios that correspond to both maximum and minimum fault conditions based on the seasons. Specifically, winter faults and summer faults, as outlined in Table 3. The resistance evolution during the fault, the maximum and minimum, and at other fault level currents are depicted in Fig. 5. For the fault current 4.9 kA the resistance evolution is very small and it is between 1.726 to 1.851 μΩ. For the other two fault currents depicted in Fig. 5, their value is in mΩ range. The $\Delta R(\frac{m\Omega}{km})$ is the change in the sequence resistance value from the steady state condition to the fault condition, provided by Nexans. The phase impedance of the HTS cable is obtained by using the equations 7 to 9. During the fault condition, this ΔR was added to Z_0, Z_1 and Z_2 to obtain the phase impedance values. While normal condition $\Delta R = 0$.

Table 3 Maximum and minimum faults during the winter and summer in the UK network

Winter/Summer	Conventional/HTS	Birkenhead-Listerdrive Fault levels	
		Current for Fault at Birkenhead, (kA)	Current for Fault at Listerdrive, (kA)
Winter Maximum	Conventional Cable	7.6	6.3
	HTS	22.4	14.7
Summer Minimum	Conventional Cable	7.1	4.9
	HTS	15.2	10

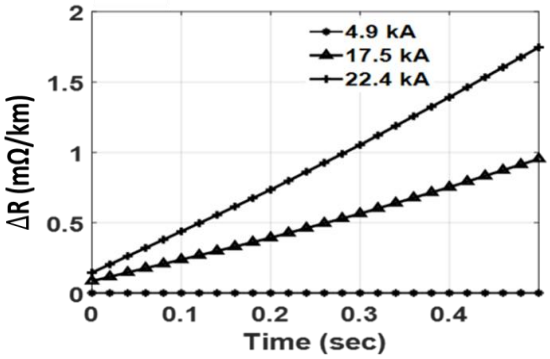

Fig. 5. HTS cable resistance evolution versus the fault duration up to 500 msec during different fault level conditions

III. RESULTS AND DISCUSSION

To assess the performance of the differential protection

principle, we conducted simulations involving various internal faults within the protected HTS circuit, including those occurring at circuit terminals and the midpoint. A fault resistance of 100 Ω was simulated to ensure compliance with protection standards in the UK. Additionally, we simulated an external fault scenario to assess protection selectivity. The outcomes of these differential protection case studies are briefly presented in Table 4.

The differential protection principle as described by (12)-(14) is not influenced by the HTS cable dynamic impedance and the results indicate that it provides dependable and selective protection for HTS cables. Differential protection however requires relays at each terminal of the protected circuit and communication between local and remote relays. Communication link failure therefore presents a risk to the dependable operation of the HTS circuit.

Table 4 Differential Protection Case Studies

Case Number	Fault Level Birkenhead (kA)	Fault Level Listerdrive (kA)	Internal / External Fault	Fault Type	Fault Location	Differential Protection Operates
1	22.4	14.7	Internal	AG	0	Y
2	22.4	14.7	Internal	AG	50	Y
3	22.4	14.7	Internal	AG	100	Y
4	22.4	14.7	External	AG	-	N

To assess the performance of the distance protection principle, fault scenarios were created at three different locations along the protected circuit, specifically at 100%, 80%, and 60% of its length. Voltage and current measurements taken at the relay location were then utilized as inputs for the distance relay model, as outlined in equations (15)-(17). The details and results of the case studies are summarized in Table 5.

Table 5 Distance Protection Case Studies

Case Number	Fault Level (kA)	Fault Type	Fault Location (%)	Fault Impedance within Protected Zone	
				Conventional Cable	HTS Cable
1	22.4	ABC	100%	Y	Y
2	4.9	ABC	100%	Y	Y
3	22.4	AG	100%	Y	Y
4	4.9	AG	100%	Y	Y
5	22.4	ABC	80%	Y	Y
6	4.9	ABC	80%	Y	Y
7	22.4	AG	80%	Y	Y
8	4.9	AG	80%	Y	Y
9	22.4	ABC	60%	Y	Y
10	4.9	ABC	60%	Y	Y
11	22.4	AG	60%	Y	Y
12	4.9	AG	60%	Y	Y

Fig. 6 illustrates the impedance plot for distance relay in the event of an HTS cable fault occurring at a location 60% along the cable's length. Notably, the fault impedance falls within the designated impedance zone characteristic, ensuring dependable relay operation. These findings confirm that distance protection can maintain reliable functionality with the given HTS cable configuration at the designated network site, and under expected operating conditions.

Under fault conditions, the HTS resistance increases according to fault level and fault duration (representing the amount of current flowing through the HTS conductor). If the temperature is below T_c, the superconductor remains superconducting; otherwise, it quenches. The increase in the current above the critical I_c values raises the resistance, resulting in temperature increases. However, the HTS reactance remains unchanged. Examining Fig. 5, the largest change in HTS resistance modelled in this study, corresponding to a fault level of 22.4 kA and fault duration of 500 ms, results in a very small HTS resistance change, ΔR. Comparing this value to the static HTS reactance shown in Table 2, it is observed to be very small, approximately 0.2% relative to the static HTS reactance. This indicates that under the specified network conditions and cable design used in the paper, the HTS cable does not experience quenching and the change in HTS impedance is dominated by the static HTS impedance. This mitigates against the potential impact of the varying HTS fault resistance.

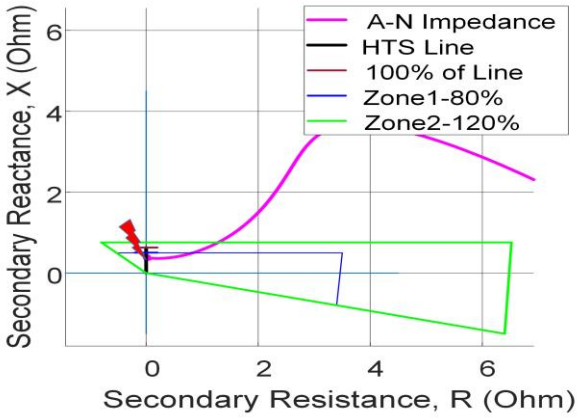

Fig. 6. Distance Case 11: AG Fault at 60% of HTS cable, AG Fault, Fault Level = 22.4kA

IV. CONCLUSION

This paper assesses the impact of HTS cables on typically applied AC protection systems. An HTS cable model incorporating the time-varying resistance under fault conditions was modelled using a manufacturer design based on a specified network location. The HTS cable model was incorporated into an equivalent network model of the specified network location. This test system was used to assess the performance of distance and differential relays which are typically adopted primary and secondary protection methods applied in the UK, respectively. Simulation case studies under a site-specific range of fault levels and fault conditions were performed. Differential protection provided dependable and selective performance. The results and accompanying analysis of the HTS cable properties show that under the specified conditions quenching does not occur and under such conditions, distance protection can be set based on superconducting impedances. The findings show that HTS cable design influences the performance of AC protection methods. Future works can include the assessment and investigation of different HTS cable designs and novel protection methods. This will allow system planners to update grid codes, and protection settings guidelines and provide valuable insights into the adoption of HTS technologies.

REFERENCES

[1] C. Lee, J. Choi, H. Yang, M. Park, and M. Iwakuma, "Economic evaluation of 23 kV tri-axial HTS cable application to power system," *IEEE Transactions on Applied Superconductivity*, vol. 29, no. 5, Aug. 2019, doi: 10.1109/TASC.2019.2908608.

[2] H. Yumura *et al.*, "Phase II of the albany HTS cable project," in *IEEE Transactions on Applied Superconductivity*, Jun. 2009, pp. 1698–1701. doi: 10.1109/TASC.2009.2017865.

[3] S. J. Lee and H. S. Yang, "Recent progress and design of three-phase coaxial HTS power cable in Korea," *IEEE Transactions on Applied Superconductivity*, vol. 29, no. 5, Aug. 2019, doi: 10.1109/TASC.2019.2908616.

[4] S. J. Lee, M. Park, I. K. Yu, Y. Won, Y. Kwak, and C. Lee, "Recent Status and Progress on HTS Cables for AC and DC Power Transmission in Korea," *IEEE Transactions on Applied Superconductivity*, vol. 28, no. 4, 2018, doi: 10.1109/TASC.2018.2820721.

[5] M. Stemmle, F. Merschel, M. Noe, and A. Hobl, "AmpaCity - Installation of advanced superconducting 10 kV system in city center replaces conventional 110 kV cables," in *2013 IEEE International Conference on Applied Superconductivity and Electromagnetic Devices, ASEMD 2013*, IEEE Computer Society, 2013, pp. 323–326. doi: 10.1109/ASEMD.2013.6780785.

[6] X. Chen, Z. Pang, M. Zhang, S. Jiang, J. Feng, and B. Shen, "Techno-economic study of a 100-MW-class multi-energy vehicle charging/refueling station: Using 100% renewable, liquid hydrogen, and superconductor technologies," *Energy Convers Manag*, vol. 276, Jan. 2023, doi: 10.1016/j.enconman.2022.116463.

[7] Z. Zheng *et al.*, "Hybrid energy transmission for liquefied shale gas and electricity using cryogenic and superconducting technologies: A technical and economic study of Sichuan, China," *Fuel*, vol. 333, Feb. 2023, doi: 10.1016/j.fuel.2022.126333.

[8] Y. Chen, S. Jiang, X. Y. Chen, Y. F. Wang, and T. Li, "Preliminary design and evaluation of large-diameter superconducting cable toward GW-class hybrid energy transfer of electricity, liquefied natural gas, and liquefied nitrogen," *Energy Sci Eng*, vol. 8, no. 5, pp. 1811–1823, May 2020, doi: 10.1002/ese3.634.

[9] W. Yuan, S. Venuturumilli, Z. Zhang, Y. Mavrocostanti, and M. Zhang, "Economic feasibility study of using high-temperature superconducting cables in U.K.'s Electrical Distribution Networks," *IEEE Transactions on Applied Superconductivity*, vol. 28, no. 4, Jun. 2018, doi: 10.1109/TASC.2018.2799332.

[10] S. Klöppel, A. Marian, C. Haberstroh, and C. E. Bruzek, "Thermo-hydraulic and economic aspects of long-length high-power MgB2 superconducting cables," *Cryogenics (Guildf)*, vol. 113, Jan. 2021, doi: 10.1016/j.cryogenics.2020.103211.

[11] E. Tsotsopoulou, A. Dysko, and D. Tzelepis, "Assesment of over-current protection for superconducting cables," 2022.

[12] M. Yazdani-Asrami, S. Seyyedbarzegar, A. Sadeghi, W. T. B. de Sousa, and D. Kottonau, "High temperature superconducting cables and their performance against short circuit faults: current development, challenges, solutions, and future trends," *Supercond Sci Technol*, vol. 35, no. 8, p. 083002, 2022.

[13] E. Y. Ko, S. R. Lee, S. Seo, and J. Cho, "Impact of Smart HTS transmission cable to protection systems of the power grid in South Korea," *IEEE Transactions on Applied Superconductivity*, vol. 29, no. 5, Aug. 2019, doi: 10.1109/TASC.2019.2908611.

[14] S. R. Lee, J.-J. Lee, J. Yoon, Y.-W. Kang, and J. Hur, "Impact of 154-kV HTS cable to protection systems of the power grid in South Korea," *IEEE Transactions on Applied Superconductivity*, vol. 26, no. 4, pp. 1–4, 2016.

[15] H. Lee, B. M. Yang, and G. Jang, "The thermal relay design to improve power system security for the HTS cables in Icheon substation," *Physica C: Superconductivity and its Applications*, vol. 494, pp. 280–285, 2013, doi: 10.1016/j.physc.2013.04.032.

[16] E. Tsotsopoulou *et al.*, "Time-domain protection of superconducting cables based on artificial intelligence classifiers," *IEEE Access*, vol. 10, pp. 10124–10138, 2022.

[17] "The Grid Code, Issue 6, Revision 18. National Grid Electricity System Operator Limited, 2023. ," *https://www.nationalgrideso.com/industry-information/codes/grid-code-gc/grid-code-documents*.